

## Impact of High-Efficiency and Variable-Speed Motors on the Performance of a Residential Split-System Air Conditioning System

John K. BREHM<sup>1\*</sup>, Florian R. RADITSCH<sup>1</sup>, Rick HEPPELA<sup>2</sup>, Davide ZIVIANI<sup>1</sup>, Eckhard A. GROLL<sup>1</sup>

<sup>1</sup>Ray W. Herrick Laboratories, School of Mechanical Engineering, Purdue University, West Lafayette, IN, USA

<sup>2</sup>QM Power, Inc.,  
Kansas City, MO, USA

\* Corresponding Author

brehm3@purdue.edu; fraditsc@purdue.edu; rhepperla@qmpower.com; dziviani@purdue.edu; groll@purdue.edu

### ABSTRACT

In the current marketplace, most of the ducted split-type heat pump systems feature single-speed compressors and fans. To meet forthcoming minimum energy rating requirements, reduce operational costs of the heat pumps, and increase environmental sustainability, the seasonal heating and cooling efficiencies of heat pump systems must be improved. Variable-speed equipment offers significant advantages for load modulation and has the ability to increase the seasonal performance greatly. Additionally, novel electrical motor technologies, such as permanent magnet (PM) motors, can reduce the power consumption of the motors by up to 25-55% compared to the widely used permanent split capacitor (PSC) motor and electronically commutated (EC) motor.

In this study, a low cost ducted single-speed heat pump system with a cooling capacity of 10.55 kW and a SEER rating of 14 BTU/Wh was analyzed to quantify the impact of fan and compressor motor efficiency on seasonal coefficient of performance (SCOP). Furthermore, the performance increase by replacing the single-speed components with state-of-the-art variable-speed equipment was evaluated. The single-speed heat pump was experimentally tested, and the results were used to tune a detailed simulation model for further performance analyses. The efficiency was evaluated in heating and cooling mode according to AHRI standard 210/240 (2023).

The conversion of the of the fan motors to high efficiency PM magnet motors increased the SCOP by 3% to 7%. The impact was dependent on the initial motor efficiency and the operational mode, where the indoor unit fan motor had a large impact on SCOP in cooling mode and a low impact in heating mode because of the motor waste heat impact on capacity. The conversion to a fully variable-speed system greatly increased the cooling SCOP by 72% and the heating SCOP by 19%.

In conclusion, current entry level ducted split systems are equipped with low efficiency PSC and EC motors, which efficiency can be increased by an upgrade to state-of-the-art PM motors, leading to an SCOP increase under low development efforts.

### 1. INTRODUCTION

Increased awareness of global warming and the rise of electricity costs are some of the main drivers to reduce energy consumption. Approximately 10% of the entire U.S. electricity consumption comes from cooling buildings alone (US Energy Information Administration, 2022), which brings the energy efficiency of heat pumps in the forefront of U.S. policymakers. Minimum energy requirements for residential heat pumps are created by the U.S. Department of Energy (DOE) and other governmental institution worldwide, to get inefficient heat pumps off the market. Due to low initial investment costs, the market is dominated by these low efficiency heat pump systems, which feature single-speed components and electric motors in the lower efficiency range (William Goetzler et al., 2013). The efficiency of these heat pumps must be increased to meet the forthcoming minimum energy requirements.

One way of increasing the systems efficiency is converting the electric motors to high efficiency motors. The indoor unit (IDU) fan motor and the outdoor unit (ODU) fan motor, typically operate with permanent split capacitor (PSC)

or electronically commutated (EC) motors, which have motor efficiencies in the range of 35% to 80% (William Goetzler et al., 2013). Replacing these motors with state-of-the-art motors can significantly reduce losses. Permanent magnet (PM) motors, which are so far not often used in residential HVAC, are currently available on the market with efficiencies of over 90% (QM Power, 2021), providing a great opportunity to increase the heat pumps efficiency.

A further change of the motors to variable-speed or multi-speed can significantly improve the systems seasonal coefficient performance due to their inherent ability to adjust their capacity to varying loads. Single-speed systems generally run in an oversized condition because the heat pump is chosen for the highest use case, which is only reached a few days a year. Most of the time, a much lower heating or cooling capacity is needed and the unit cycles on-off, which results in inefficiencies. A variable-speed system can overcome these losses by adjusting its capacity to the required load. Additionally, at lower speeds, the heat transfer often is enhanced, which further increases the efficiency.

This work investigates the performance improvements of heat pump systems when (1) upgrading the indoor unit fan motor and outdoor fan motor to state-of-the-art high efficiency motors and (2) upgrading single-speed motors to variable-speed motors.

## 2. SYSTEM DESCRIPTION

### 2.1 Baseline Unit

In this study, a low-cost commercially available ducted single-speed heat pump system was evaluated. The system was rated with a seasonal coefficient of performance of 4.1 (equivalent to SEER 14 BTU/Wh) according to AHRI Standard 210/240 (2017). The heat pump was equipped with a single-speed scroll compressor and used the refrigerant R410A, which is the standard in the U.S. for this application. The cooling capacity was stated as 10.55 kW by the manufacturer. The indoor unit fan was operated with a 0.5 HP EC motor and the outdoor unit fan was operated with a 0.2 HP PSC motor. Both fans were operated at a single speed.

The motor efficiencies of the baseline motors were not provided. With experimental results and the fan motor curves from the high efficiency motors, the baseline fan motor efficiencies were back calculated with equation 1. The tests were performed at same operating speed and torque, and therefore, at same shaft power.

$$\eta_{Baseline} = \eta_{PM} * \frac{P_{fan,PM}}{P_{fan,Baseline}} \quad (1)$$

With this calculation, the baseline IDU fan ECM was estimated to have a motor efficiency of 73% and the baseline ODU fan PSC motor an efficiency of 58%.

### 2.2 High Efficiency Fan Motors

The baseline evaporator fan and condenser fan motors were converted to state-of-the-art variable-speed permanent magnet motors. These motors use the novel Q-Sync speed control (QM Power, 2021), which uses AC-to-AC conversion that eliminates traditional AC to DC conversion components, yielding significant reductions in energy usage. The speed was adjusted with a pulse-width-modulation (PWM) controller in the test setup. The motor efficiencies for the high efficiency PM are shown in Figure 1. The efficiencies were determined from bench tests and were provided by the motor manufacturer (QM Power, 2021). Moreover, Figure 1 also reports the baseline EC and PSC motor efficiency assumptions which were calculated with Equation 1. The plot shows the significant improvement potential of the fan motors with the efficiency increasing by up to 52%.

### 2.3 Variable-speed Conversion

The heat pump was converted to variable-speed by replacing the single-speed compressor of the baseline unit with a state-of-the-art variable-speed compressor. The compressor remained a hermetic R410A scroll compressor, with the ability to modulate its speed. The maximum capacity of the compressor was very similar to the rated capacity of the single-speed compressor, with a rated capacity range of 2.64 kW to 10.75 kW.

### 2.4 Other Modifications to the Unit

The unit was equipped with a mass flow meter and multiple thermocouples and pressure transducer to assess the operating conditions. Additionally, the baseline unit expansion devices were upgraded with electronic expansion valves (EEV), to maintain sufficient superheat in all operating conditions. In this study, the with EEVs modified heat pump was considered as the baseline.

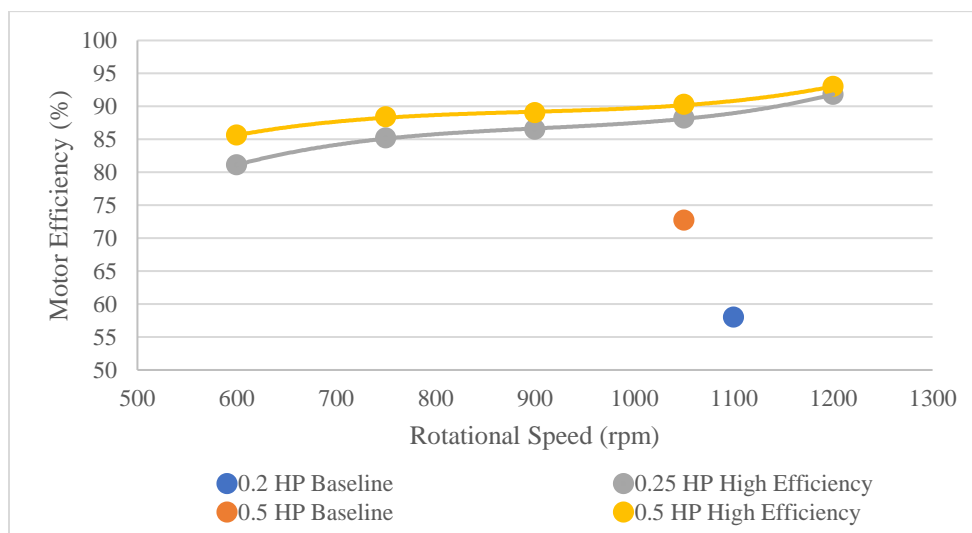


**Figure 1:** Motor Efficiency of the single-speed baseline motor and the high efficiency variable-speed PM Motor

### 3. METHODS

The efficiency of the heat pump was experimentally evaluated in different configurations. Each configuration was tested in both cooling and heating modes. The modifications to the heat pump to improve its efficiency, as described in Section 2, were done step-by-step to assess the impact on system efficiency of each component. The experimentally obtained results were then used to tune a simulation model, to further assess the impact of motor efficiencies and variable-speed operation on system efficiency.

#### 3.1 Efficiency Evaluation

The efficiency of the heat pump was evaluated by calculating the seasonal coefficient of performance for cooling ( $SCOP_C$ ) and the seasonal coefficient for heating ( $SCOP_H$ ). The coefficients were evaluated with the AHRI Standard 210/240 (2023), which is the standard used by industry in the U.S. to rate residential split system heat pumps. The SEER2 value from the standard was converted to the unitless  $SCOP_C$  value and the HSPF2 value was converted to the unitless  $SCOP_H$  value for consistency with the SI unit system.

The methods in the standard attempts to replicate the operation of a heat pump over a cooling or heating season and determines the average coefficient of performance (COP) of the unit within the season. These coefficients are a reasonable indicator of the system's performance as they consider the efficiency under many different operating conditions that are expected in a cooling or heating season.

The standard differentiates between single-speed heat pump and variable-speed heat pump systems. Hereby, the standard employs additional tests for the variable-speed systems to characterize their operation under varying loads. Depending on the outdoor condition and capacity needs, the compressor and fans of the variable-speed system operate at either full speed, intermediate speed or a low speed.

The  $SCOP_C$  or  $SCOP_H$  was calculated with temperature bins that display the expected temperature within a year of operation and the information of capacity and power consumption at the different operation points.

The standard has optional tests, to assess losses which occur during cycling of the compressor. These losses were accounted for with the degradation coefficient  $C_d$  (AHRI, 2023). In this study, these optional tests were not conducted and hence per standard, a constant coefficient of 0.2 was taken for single-speed systems in cooling mode and 0.25 for all other systems and operational modes to calculate the  $SCOP_C$  and  $SCOP_H$ .

#### 3.2 Experimental Testing

The heat pump was tested with the room air enthalpy test method as specified by ASHRAE Standard 37 (2019). Figure 2 shows the cycle schematic of the heat pump with sensor positions. The system is installed in two psychometric chambers side-by-side, which are able to simulate temperatures and humidity over the range of  $-20\text{ }^{\circ}\text{C}$  to  $55\text{ }^{\circ}\text{C}$ . The outdoor unit was positioned in the outdoor room, which simulated outdoor air conditions with temperatures ranging

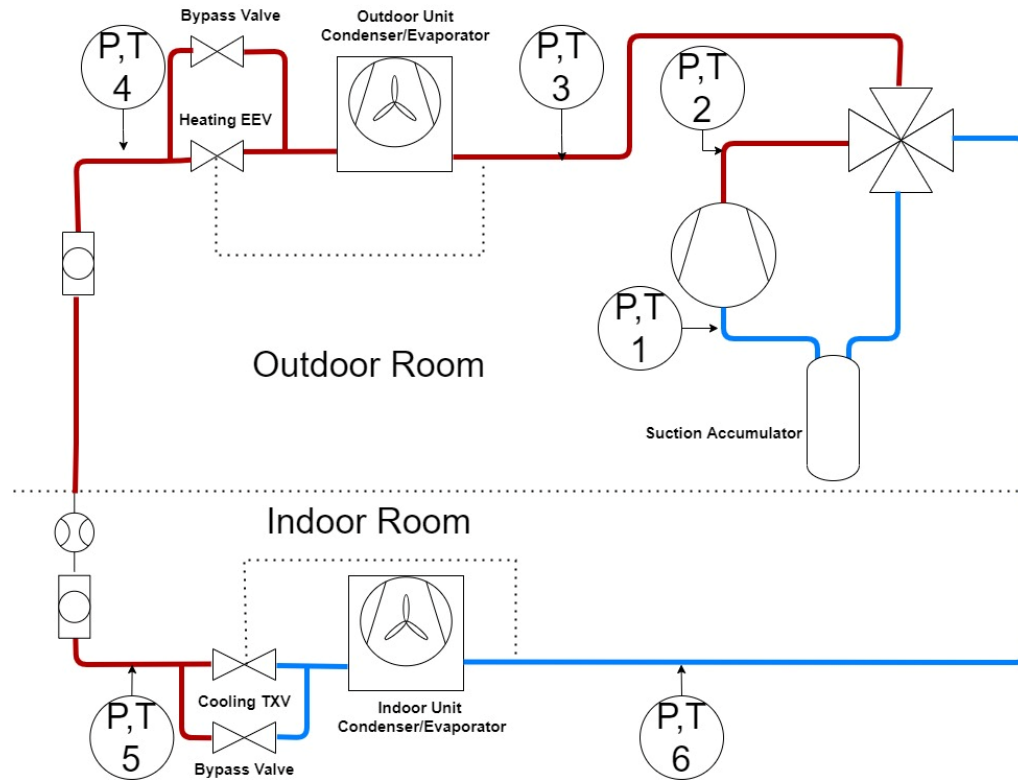


**Figure 2:** Heat pump cycle schematic with sensor positions.

from  $-8.3\text{ }^{\circ}\text{C}$  to  $35\text{ }^{\circ}\text{C}$ . The indoor unit was positioned in the indoor room, which simulated indoor air conditions, with temperatures ranging from  $21.1\text{ }^{\circ}\text{C}$  to  $26.7\text{ }^{\circ}\text{C}$ .

The capacity was measured simultaneously with both the air enthalpy method and the refrigerant enthalpy method, in order to validate the measurements. The measurements were performed following ASHRAE Standard 37 (2019). Using the air enthalpy method, the air properties at the inlet and the outlet of the indoor unit were measured. The temperature was measured using a grid consisting of 9 thermocouples. The humidity was measured at the inlet and at the outlet with a cold mirror sensor. The airflow was measured at the outlet of the duct with a nozzle airflow measuring apparatus according to ANSI/ASHRAE Standard 51 (2007). With these measurements, both the enthalpies  $h_{a1}$  and  $h_{a2}$  and specific volume  $v_n$  were calculated. The cooling capacity was then calculated with equation 2.

$$\dot{Q}_{air} = \frac{\dot{V} * (h_{a1} - h_{a2})}{v_n} \quad (2)$$

For the refrigerant enthalpy method measurements of the refrigerant were taken. A Coriolis-effect mass flow meter measured the mass flow rate  $\dot{m}_r$  at the subcooled condenser outlet section. In line thermocouples and pressure transducers at the inlet and outlet of the indoor unit heat exchanger were used to determine the enthalpies  $h_{r1}$  and  $h_{r2}$ . In cooling mode, isenthalpic expansion was assumed, and the properties were measured at the expansion device inlet. To account for the heat from the IDU fan motor, the indoor unit power  $P_{Fan,i}$  was subtracted from the capacity in cooling mode and added in heating mode. Equation 3 shows the cooling capacity calculation for the refrigerant enthalpy method:

$$\dot{Q}_{refrigerant} = \dot{m}_r * (h_{r2} - h_{r1}) - P_{Fan,i} \quad (2)$$

### 3.3 System Modeling

Numerical analyses were conducted by employing the simulation framework “ACHP+” which is coded in the Python programming language. Such modeling framework is the result of two decades of efforts by the authors’ research team in simulating various vapor compression systems. In a nutshell, ACHP+ is a detailed charged sensitive model, which assesses the influence of heat exchanger sizing, compressor efficiencies, expansion work recovery devices, working

fluids, etc. on the system's performance. The model has been experimentally validated by various studies (e.g., A. Bahman et al., 2018) giving confidence in the accuracy of the model.

The baseline single-speed scroll compressor was integrated into the ACHP+ model with a 10-coefficient polynomial map as defined by AHRI Standard 540 (2020). The coefficients for power input and the mass flow rate were developed from a compressor map, which was provided by the compressor manufacturer. The 10-coefficient polynomial map allows to calculate power and mass flow rate at the operational point with inputs of suction dew point temperature and discharge dew point temperature. For modelling the variable-speed scroll compressor, a modified 10-coefficient polynomial map was used. The compressor manufacturer provided a 20-coefficient polynomial map to additionally account for the rotational speed of the compressor.

The performance of indoor unit fan and outdoor unit fan was modeled based on experimental data and the affinity laws. The rotational speed, airflow and power consumption of both indoor unit and outdoor unit fan were validated with experimental data over a wide range of operational speeds and for different operating conditions.

The model was tuned for charge with a two-point method, developed by Shen et al. (2006). In addition to the charge, 7 tuning multipliers were investigated to account for mass flow rates, heat transfer coefficients and pressure drops on the air-side and refrigerant side. This tuning method was proposed by Bahman et al. (2018), to reduce the deviation to experimental results, which resulted from simplifications and imperfect information within the model.

## 4. VALIDATION

### 4.1 Experimental testing

The baseline measurement results were compared with the efficiency data provided by the heat pump manufacturer. The system is rated with an  $SCOPI_C$  of 4.1 and an  $SCOPI_H$  of 2.4 according to AHRI standard 210/240 (2017). In the baseline configuration, an  $SCOPI_C$  rating of 4.02 and an  $SCOPI_H$  of 2.24 was measured. Hereby, the  $SCOPI_C$  rating is very close to the manufacturer data. The deviation might be a result of the assumed degradation coefficient  $C_d$ . Because additional optional tests were not conducted in this study, this factor is likely overpredicted. Moreover, an  $SCOPI_C$  was measured with a higher static pressure across the fan coil to match the requirements of the 2023 version of AHRI standard 210/240 which also impacted the results in this comparison.

The measured  $SCOPI_H$  deviates from the manufacturer data to some extent. This can be explained by the modification of the expansion device. In the unmodified unit in heating mode, a short orifice was used as an expansion device. No superheat was achieved, and the suction line accumulator collected charge and prevented liquid to reach the compressor. With the modification of an EEV in the baseline unit, superheat at the evaporator outlet was achieved, which indicates that the accumulator did not collect any charge. Due to different heat exchanger sizes of the outdoor unit and indoor unit, excessive charge relocated into the condenser due to no charge compensation within the accumulator in heating mode. This led to a high degree of subcooling of approximately 19 K which reduced the measured efficiency as compared to the manufacturer data.

Additionally, the capacity measurements were validated by comparing the capacity measured with the refrigerant enthalpy method and the air enthalpy method. According to the standard, this deviation must be below 6%. The measured capacity as well as the deviation for different test conditions are shown in Figure 4. All test conditions had a deviation below 6% indicating that the measurements were accurate and reliable.

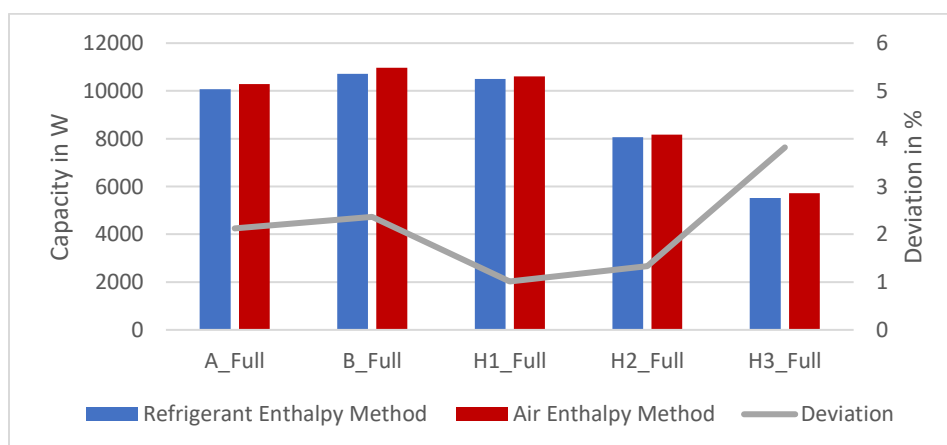


**Figure 4:** Comparison and deviation of capacity measurement between the refrigerant enthalpy method and air enthalpy method

## 4.2 System Modeling

The simulation model was validated with results obtained through experimental testing. In the baseline configuration in cooling mode, the system model agreed extremely well with the test results. Table 1 lists a selection of important system operational values for both the experiment and the model in cooling mode. The  $SCOP_C$  value deviates by 0.4% between the experiment and the system model. The rated capacity matches almost identically. Similarly, important heat exchanger parameters, such as condensation temperature, evaporation temperature, subcooling and superheat match closely with experimental data. The fan power consumption matches near perfectly with experimental data, as the model's fan curves were based on experimental data. Overall, the comparison in cooling mode shows that the model is accurate and that the tuning was successful.

Similarly, the results for operation in the heating mode were compared. The modeled results deviate from the experiment more than in the cooling mode with a deviation of 23.8% in  $SCOP_H$ . A large deviation in condensing temperature of 8.4 K and subcooling of 9.8 K suggests that the charge tuning was not accurate for operation in heating mode. The charge was likely underpredicted, as a larger charge would result in a higher subcooling and higher condensing temperature. Due to the lower pressure ratio that the compressor must overcome, the compressor power was underpredicted in the model, which partly explains the 23.76% deviation in  $SCOP_H$ . The large subcooling of 19 K in the experimental test setup, is not expected to occur in the field, as a properly designed heat pump would account for the relocation of refrigerant and compensate the charge with either an accumulator or receiver. This compensation did not occur in the tested baseline unit, due to the conversion to electronic expansion valves. As a result, it was decided to run the model with the charge tuning factors obtained from operation in cooling mode. The results from the model are not directly comparable with the experimental results, however, it is expected that the model results give meaningful predictions as the operating conditions are closer to the real use case in the field.

The modeling results of the variable-speed system were not validated due to lack of experimental results. The high agreement of the results in cooling mode of the baseline system suggests that the model can be trusted to extrapolate results for operation with a different compressor.

**Table 1:** Comparison of the baseline experimental results and modeling results in cooling mode

	Experimental Testing	ACHP+	Deviation
$SCOP_C$	4.02	4.03	0.36%
$A_{full}$ cooling capacity	10147 W	10212 W	0.64%
$B_{full}$ cooling capacity	10836 W	10907 W	0.66%
$B_{full}$ massflow	62.27 g/s	61.62 g/s	-1.04%
$B_{full}$ condensation temperature	36.2 °C	36.1 °C	-0.1 K
$B_{full}$ evaporation temperature	9.5 °C	10.7 °C	1.2 K
$B_{full}$ subcooling	4.3 K	5.0 K	-0.7 K
$B_{full}$ superheat	7.5 K	7.5 K	0.00 K
$B_{full}$ ODU fan power	192 W	191 W	-0.21%
$B_{full}$ IDU fan power	377 W	377 W	0.27%
$B_{full}$ compressor power	1860 W	1914 W	0.58%

## 5. RESULTS

### 5.1 Single-Speed Heat Pump

Figure 5 shows the modeled  $SCOP_C$  of the heat pump in different configurations. By changing the ODU fan motor to a high efficiency motor, the system efficiency increased by 2.8%. The further change to a more efficient IDU motor had a larger impact on  $SCOP_C$  and increased the system efficiency by 6.6% compared to baseline. Figure 6 displays the power savings of each fan motor. The IDU fan motor relative savings were larger than the relative savings of the ODU fan motor. However, the absolute savings were relatively similar with savings of 64 W (ODU) and 70 W (IDU). Figure 7 shows the modeling results for operation in heating mode. The upgrade to higher efficiency ODU fan motor increased the  $SCOP_H$  by 2.2%, which is similar to the finding in cooling mode. The further upgrade of the IDU fan motor had a much smaller impact than in cooling mode, increasing the  $SCOP_H$  by 3% over baseline. Figure 8 shows the power savings of the motors, which are similar to the savings measured in cooling mode. Here, the IDU fan motor power savings were slightly reduced which could be either due to a more efficient operational condition of the baseline motor or a less efficient operational condition of the PM motor.

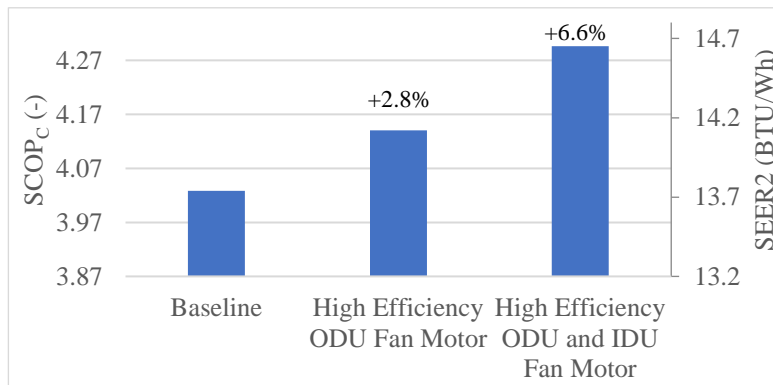


Figure 5: Modeled SCOP<sub>C</sub> in different configurations

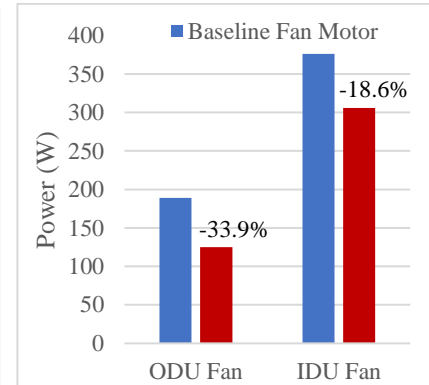


Figure 6: Fan power at B<sub>Full</sub> condition

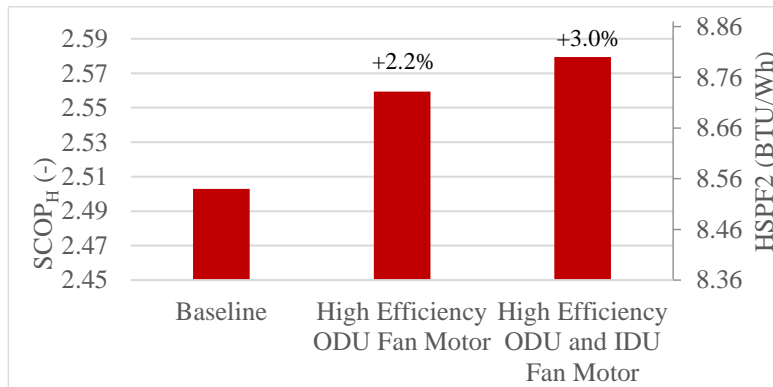


Figure 7: Modeled SCOP<sub>H</sub> in different configurations

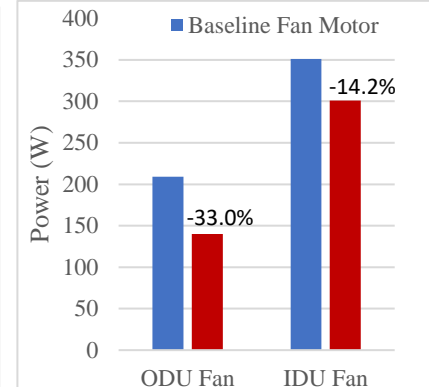


Figure 8: Fan power at H1<sub>Full</sub> condition

## 5.2 Variable-Speed Heat Pump

To assess the impact of variable-speed systems in different configurations, an analysis with a variable-speed compressor was conducted. For a fair comparison of efficiency between the operating modes, independent of compressor efficiency, the baseline single-speed compressor in this section is the same variable-speed compressor but operating at a single-speed of 4500 rpm, which is the rated speed. The variable-speed compressor is labeled as “high efficiency” compressor and the operational mode is indicated by the abbreviation SS for single-speed operation and VS for variable-speed operation. At each configuration in variable-speed mode, the compressor, IDU fan and ODU fan speed was optimized at low speed and intermediate speed.

Figure 9 shows the SCOP<sub>C</sub> in different configurations. The system efficiency of the system with the high efficiency compressor operating in single-speed (configuration 1) is 8.0% lower than the SCOP<sub>C</sub> of the baseline system with dedicated single-speed compressor. In configuration 3 in variable-speed mode with single-speed fans, the SCOP<sub>C</sub> was 15.3% higher. While generally, the fan power makes up only a small portion of the heat pumps total power (<20% in the single-speed configuration), in configuration 3, the fan power is the dominating power at the low speed tests. By converting both fans to operation in variable-speed, the SCOP<sub>C</sub> increased by 71.9% compared to SS operation. After the conversion to variable-speed fans, the portion of fan power to total power decreased significantly.

The results for SCOP<sub>H</sub> in different configurations are shown in Figure 10. The conversion to variable-speed compressor and single-speed fans (configuration 3), increased the SCOP<sub>H</sub> by 6.3% compared to baseline configuration 1. The change of the IDU fan to variable-speed, increased the efficiency to 10.5%. The further conversion of the ODU fan to variable-speed had the largest impact on efficiency and increased the SCOP<sub>H</sub> by 19.4%. Overall, the improvement in heating mode was much lower, than in cooling mode.

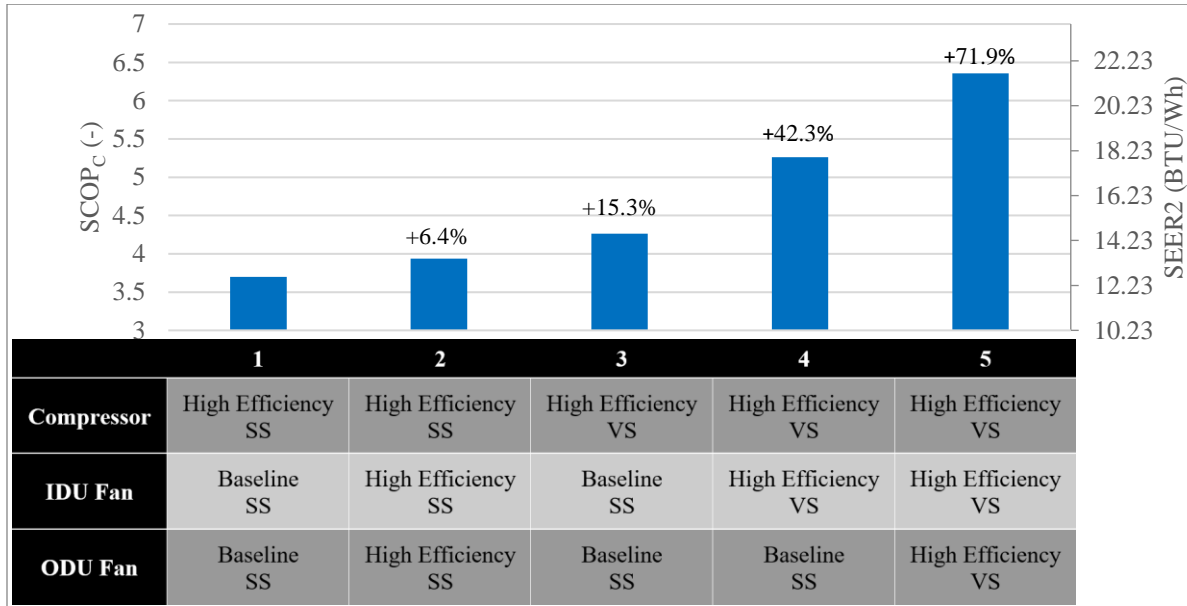


Figure 9: Modeled SCOP<sub>c</sub> in different configurations

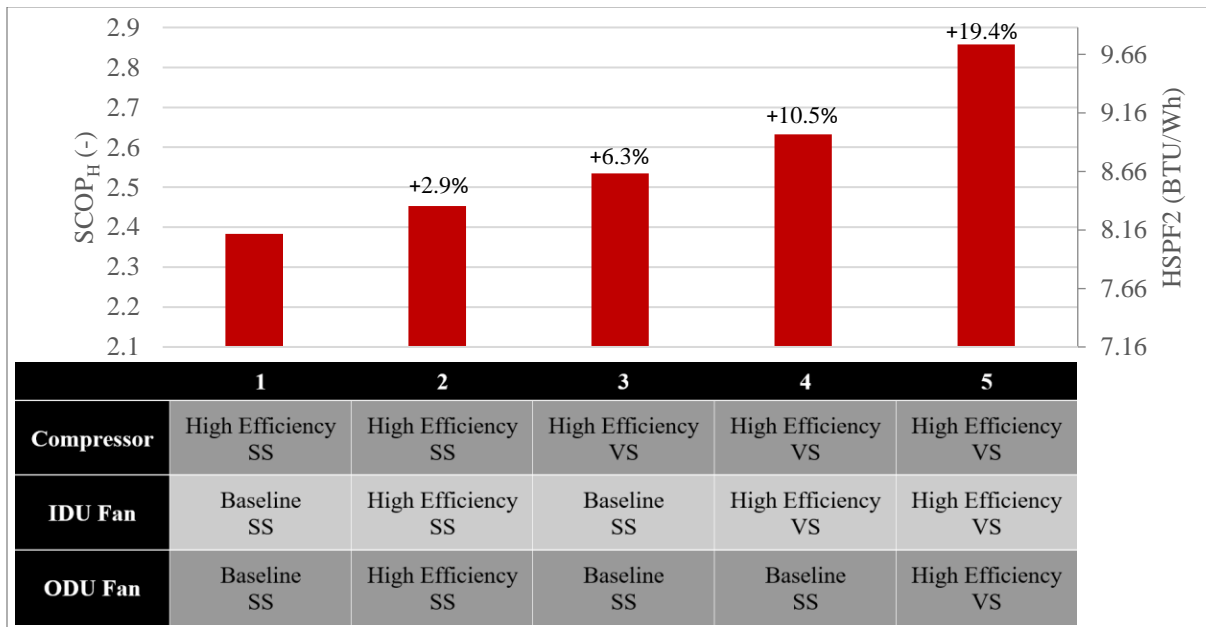


Figure 10: Modeled SCOP<sub>h</sub> in different configurations

## 6. DISCUSSION

The results showed that a high improvement can be achieved by changing the motors to high efficiency permanent magnet motors. Although the indoor unit fan motor was larger, the absolute power savings between the indoor and outdoor unit fan motor were relatively similar due to a lower efficiency of the baseline ODU fan motor.

To model the impact of each motor on SCOP, the findings were used to approximate the SCOP increase with each percentage of motor efficiency increase. The results for a single-speed system are shown in Figure 11. The compressor motor has the largest efficiency increase per percentage motor efficiency increase, which makes sense, as it is the largest power consumer within the heat pump. The compressor of the investigated system makes up roughly 80% of the total power. In heating mode, the SCOP improvement from the compressor motor was much lower than in cooling



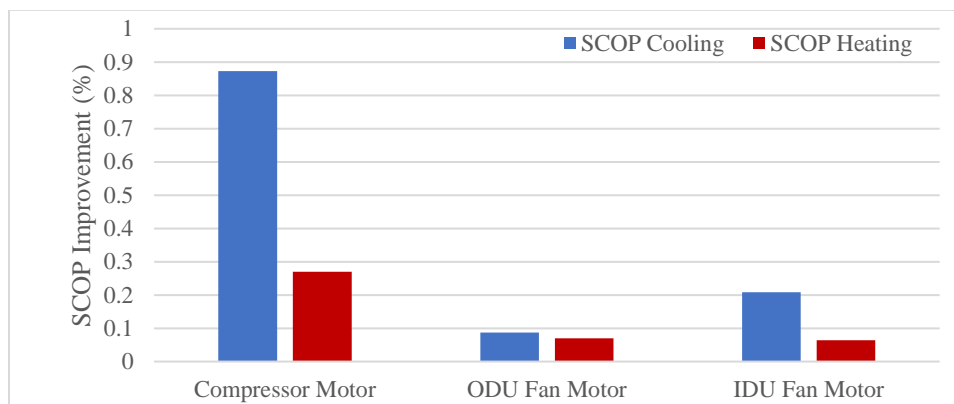


**Figure 11:** SCOP improvement in heating and cooling mode with 1% of motor efficiency increase for single-speed systems

mode. In heating mode, the improvement is lower because the waste heat of the compressor motor is useful to the heating capacity. The compressor motor efficiency increase reduces the power consumption, which increases the  $SCOP_H$ . However, this increase is partly compensated by the now reduced heating capacity, resulting in a lower SCOP increase compared to operation in cooling mode, where the waste heat is not useful for capacity.

The indoor unit fan motor efficiency increase shows a similar result with a large difference between cooling mode and heating mode improvements. Hereby, the motor waste heat gets rejected into the conditioned air. In cooling mode, this waste heat, reheats the cooled air. Due to that, a higher efficiency motor not only reduces the power consumption, but also increases cooling capacity, which greatly increases the  $SCOP_C$ . In heating mode, this additional heat is useful, and therefore, a higher efficiency motor, while reducing fan power, reduces the heating capacity. This reduces the gain compared to cooling mode. The outdoor unit fan motor improvements are similar between cooling and heating mode. This makes sense, because the ODU fan motor waste heat is rejected into the environment and hence, does not impact the refrigeration cycle itself. It is worth to mention, that generally, compressor motors already have a high efficiency. Therefore, despite the large impact on SCOP, the improvement potential is limited. The IDU fan motor and ODU generally have lower efficiencies, which offers a great opportunity for improvement. Fan motors can be easily upgraded with little development effort as these components do not directly impact the refrigeration cycle.

A similar analysis was conducted for variable-speed systems and near identical results were found. Hence, the findings shown in Figure 11 can be adapted to variable-speed components.

The conversion to operation of the compressor in variable-speed, with single-speed fans resulted in only a little increase in  $SCOP_C$  and  $SCOP_H$ . In this configuration, the fans made up a large portion of the total energy. At full speed operation, the fan power made up 20% of the total energy. At intermediate speed this portion increased to 33% and in low speed to 58%. At lower compressor speeds, the capacity is much reduced and hence less heat needs to be exchanged at the heat exchangers. As the single-speed fans cannot adjust for the lower capacity, in part load operation of the compressor, the fans operate with an airflow that is higher than necessary. The high airflow has little beneficial impact on the heat transfer, while requiring a high power input, which reduces the SCOP.

With the change of the fan motors, a large increase in  $SCOP_C$  of 72% and  $SCOP_H$  of 19% was achieved. Hereby, both fan upgrades to variable-speed had a large impact on SCOP which shows that for the investigated system, it was worth it and almost necessary to change the whole system to variable-speed components. In the fully variable-speed system, the fans now made up a much smaller portion of the total power. At intermediate speed, the fan power portion reduced from 33% to 15% and at low speed from 58% to 35% in cooling mode. In heating mode, the portion reduced from 39% at intermediate speed and 57% at low speed to 13% and 17% respectively. This shows that the fans were far from their optimum at single-speed operation.

## 7. CONCLUSIONS

This research aimed to quantify efficiency gains and energy savings by employing higher efficiency motors in a 10.55 kW ducted residential split system heat pump. Furthermore, the study aimed to quantify the efficiency gains by employing variable-speed equipment in the same unit. For the analysis the single-speed heat pump was experimentally evaluated with different fan motor configurations. The results of the single-speed heat pump were then used to tune the charge sensitive model ACHP+ and assess different configurations, such as variable-speed.

In the baseline single-speed configuration, the conversion of the fan motors to state-of-the-art fan motors significantly improved the motors efficiency and reduced fan motor power consumption by 21% (IDU fan) to 34% (ODU fan) at

same speed. Hereby, the absolute energy savings between outdoor unit fan motor and indoor unit fan motor were similar due to the larger size of the IDU fan motor. Between cooling and heating mode, the impact of outdoor unit fan motor on SCOP were similar with a gain of 0.09% (cooling) and 0.07% (heating) per percentage of ODU fan motor increase. For the indoor unit motor, the impact on SCOP increase differentiated between cooling and heating mode. This was due the negative impact of the IDU motor waste heat on cooling capacity and positive impact of the IDU motor waste heat on heating capacity. The IDU fan motor impact on SCOP<sub>C</sub> were 0.21% per percentage of motor efficiency increase and 0.06% on SCOP<sub>H</sub>. In total, the upgrade to state-of-the-art fan motors in the single-speed heat pump resulted in an increase of 6.6% on SCOP<sub>C</sub> and 3.0% on SCOP<sub>H</sub>.

The upgrade of the single-speed compressor to a state-of-the-art variable-speed compressor resulted only in little efficiency gain when the fans were not upgraded to variable-speed operation as well. The high efficiency gain due to the variable-speed compressor was prevented by the high fan power at part load operation, which made up up to 58% of the total power. The further upgrade to variable-speed fans had a large impact on SCOP by both IDU and ODU fan. The SCOP<sub>C</sub> was increased by 72% and the SCOP<sub>H</sub> by 19%. This showed that to prevent high losses, the whole system must be converted to variable-speed.

### NOMENCLATURE

ECM	Electronically commutated motor	
EEV	Electronic expansion valve	
h	Enthalpy	J/kg
HP	Horsepower	
HSPF	Heating seasonal performance factor (AHRI 210/240 2017)	BTU/Wh
HSPF2	Heating seasonal performance factor (AHRI 210/240 2023)	(BTU/Wh)
$\dot{m}$	Massflow	kg/s
P	Power	W
PM	Permanent magnet	
PSC	Permanent split capacitor	
$\dot{Q}$	Capacity	W
SCOP <sub>C</sub>	Cooling seasonal coefficient of performance, converted SEER2	(-)
SCOP <sub>H</sub>	Heating seasonal coefficient of performance, converted HSPF2	(-)
SEER	Seasonal energy efficiency ratio (AHRI 210/240 2017)	(BTU/Wh)
SEER2	Seasonal energy efficiency ratio (AHRI 210/240 2023)	(BTU/Wh)
SS	Single-speed	
VS	Variable-speed	

### REFERENCES

- AHRI. (2017). *Standard 210/240: Performance Rating of Unitary Air-conditioning & Air-source Heat Pump Equipment*.
- AHRI. (2020). *Standard 540: Performance Rating of Positive Displacement Refrigerant Compressors*.
- AHRI. (2023). *Standard 210/240: Performance Rating of Unitary Air-conditioning & Air-source Heat Pump Equipment*.
- ANSI/ASHRAE. (2007). *Standard 51: Laboratory Methods Of Testing Fans For Aerodynamic Performance Rating*.
- ASHRAE. (2019). *Standard 37: Methods of Testing for Rating Electrically Driven Unitary Air-Conditioning and Heat-Pump Equipment*. [www.ashrae.org/technology](http://www.ashrae.org/technology).
- Bahman, A., Ziviani, D., & Groll, E. (2018, July 9). *Development and Validation of a Mechanistic Vapor-Compression Cycle Model*.
- QM Power. (2021). *Q-Sync® HVAC Permanent Magnet Synchronous Fan Motors Q-Sync® HVAC 1/2Hp 60Hz PRODUCT SPECIFICATIONS*. [www.qmpower.com](http://www.qmpower.com)
- Shen, B., Braun, J. E., & Groll, E. A. (2006). A Method for Tuning Refrigerant Charge in Modeling Off-Design Performance of Unitary Equipment (RP-1173). *HVAC&R Research*, 12(3), 429-449. <https://doi.org/10.1080/10789669.2006.10391188>
- US Energy Information Administration. (2022). *Annual Energy Outlook 2022*. [www.eia.gov](http://www.eia.gov)
- William Goetzler, Timothy Sutherland, & Callie Reis. (2013). *Energy Savings Potential and Opportunities for High-Efficiency Electric Motors in Residential and Commercial Equipment*. <http://www.osti.gov/home/>

### ACKNOWLEDGEMENT

The authors would like to thank QM Power for sponsoring this research project.